Comparison of methods for separating flood frequency of reservoir by sub-seasons

Jiqing Li[1], Kaijie Xie[1], Mingjiang Xie[1]and Rongbo Li[1]

[1]{School of Renewable Energy, North China Electric Power University, Beijing, China}

Correspondence to: Jiqing Li (jqli6688@163.com jqli6688@ncepu.edu.cn)

Abstract

The development of separate flood frequency distributions for different sub-seasons within a year can be useful for protection, storage and utilization of flood flows for the reservoir operation management. This paper applies conventional statistical method, fractal method and the mixed Von Mises distribution to the separation of flood sub-seasons for inflows to Hongfeng Reservoir in China. Design floods are found for different sub-seasons, along with flood control levels for flood regulation. The flood season is divided into four sub-seasons using the fractal method: the pre-rainy season (May), main-flood season (June and July), late-flood season I (August) and late-flood season II (September). The mixed Von Mises distribution method accounts for the general flood pattern and combines August and September as one late-flood season, for three sub-seasons with different frequency distributions. The flood regulation calculation results show little difference between the control water levels in August and September, so the two can be combined into one period. Due to flood regulation and generation caculation, varied sub-season flood limited water level are able to obtain more economic benefits without decreasing the original flood prevention standard. Therefore, flood season separation is significant in calculating design floods of different stages and determining flood control levels, allowing better reservoir operation within different flood sub-seasons.

1 Introduction

Increasing water demands have intensified water scarcity in China. Reservoirs have a significant role in resolving the tension between the water supply and demand. To fully use

flood resources and reduce water shortages, many researchers propose increased "floodwater utilization" (Cao, 2004). Floodwater utilization focuses on effective flood management through analyzing seasonal variation of floods with flood-control safety, where reasonable separation of the flood season is a key for better benefit. Regulation for calculating design flood of water resources and hydropower projects of China requires that flood season separation should consider the design requirements of projects, and have appropriate flood timing according to seasonal varying flood patterns. This means design floods of different sub-seasons should be calculated based on flood characteristics for project design for practical construction and operation. However, according to the Chinese Flood Control Act, the reservoir flood limited water level which is determined bythe reservoir routing of the annual design flood hydrographs, should not be kept high during the flood season to offer adequate storagefor flood prevention. Meanwhile, the designed flood, based on the annual maximum sample, neglects flood seasonality, and hence, the conventional flood limited water level is often a fixed value during the entire flood season. Based on the flood seasonality, separation of flood season of reservoir is to make better flood regulation schemes, which can make better use of the surplus water in flood season and increase benefits, such as by generating more electricity, without extra construction cost. Therefore, the statistical development of flood frequencies for sub-seasons within the annual flood season has potential to improve multipurpose reservoir system operation.

Flood operations of reservoirs are commonly for a single defined “flood season”, differing from the remainder of the year when floods are unlikely to occur. Many methods can help define the flood season, and to define how flood operations might vary in sub-seasons within the flood season. Many new methods also are available, such as fuzzy analysis, changing point analysis, fractal theory method etc. Chen (1995) proposed a fuzzy set application to flood season definition, reflecting fuzziness of flood season boundaries in time. The fuzzy membership functions used to separate flood season and non-flood season are derived statistically, and the flood control level is calculated daily in the transition period to improve water utilization. Liu et al. (2005, 2015) introduced the theory of changing point analysis and detailed the theory and analytical method of mean changing point and probabilistic changing point in flood sub-seasons for the Three Gorges Reservoir. Hou et al. (1999) used fractal theory to analyze flood peak sequence and studied flood sub-seasons for Xiaodeshi Station in China. The result of the fractal method is consistent with conventional empirical results. But the new method is less subjective. Fang et al. (2007) reviewed flood sub-season analysis

methods and discussed their comparative advantages and disadvantages. Fang et al. (2008) used the Von Mises distribution as the annual maximum flood time distribution function to describe flood physical laws, and provided a new method for determining sub-seasonal design floods. Wei et al. (2014) used fractal theory in the study of flood sub-seasons for Bihe Reservoir. Because flood frequency distributions can be multimodal, Chen et al. (2010) used a mixed Von Mises distribution varying with flood date and derived sub-season varying design floods.

This paper is mainly concerned about the separation of flood season, analyzes the flood characteristics of Hongfeng Reservoir as an illustrative example, and divided its flood season into different sub-seasons using statistical method, fractal theory and a mixed Von Mises distribution. Seasonal design floods and flood control levels of different sub-seasons were then calculated according to the developed flood operating rules and strategies. Based on the flood regulation calculation in sub-seasons, the different ranges of flood control level in each sub-season are obtained with the fixed flood control level of the original plan as the lower limit. Under the requirement of flood control safety, adopting the new operation schemes can help increase the total benefits of reservoir, especially in electricity generation and water supply, etc.

2 Methods of flood season separation

The first conventional statistical method used in this paper is a basic one to separate annual flood season, which calculate the accumulative frequencies in flood-prone period and then obtain the separation result.

2.1 Statistical method----conventional method

To separate a flood season into sub-seasons, the physical cause of the flood should be analyzed considering the meteorological and hydrologic characteristics of the studied river. Then according to the allocation pattern of rainfall and flood within a year and the inflow records of the representative hydrologic station, the flood frequency with given magnitude can be obtained. Generally, the physical cause of the flood and the hydrologic characteristics of the river should be analysed first. According to the allocation pattern of rainfall and flood and the inflow records for certain reservoir, the actual time and Cumulative probability of the first, second and third largest flood peaks of all the largest inflows occurring should be

obtained under the time scale of month or ten-day period. Next, based on the calculated frequencies, the separation of the flood season can be determined based on the seasonal changing pattern of the flood in combination with the analysis of rainfall characteristic, storm characteristic, atmospheric circulation and other relevant meteorological factors.

2.2 Fractal theory method

The Fractal method focuses on the fractal dimension of each sub-season. With an assumed time length of a sub-season, its fractal dimension can be obtained. When prolonging the time length of the sub-season, a different fractal dimension can be obtained and by comparing these two fractal dimensions it can be determined whether the time length of the sub-season is the prolonged one based on self-similarity. Then the whole flood season can be separated into several sub-seasons based on different fractal dimensions.

2.2.1 Fractal theory

A fractal is a natural phenomenon or a mathematical set that has a repeating pattern at every scale, featured with self-similarity and scale-invariance. Fractal theory was established by B.Mandelbrot in the 1970s. It has been applied to many areas, including philosophy, mathematics, chemistry, physics, economics, geology, seismology, geography, music, and art (Liu et al., 2006). Fractal theory has been applied to hydrology and water resources, such as the fractal of morphological characteristics of watershed systems, the longitudinal channel profile, and flood forecasting and flood disaster prediction (Zhang et al., 2009). Zhang et al. (2009) also have applied fractal theory to developing flood sub-seasons.

The current study of fractal is based on the qualitative understanding of the examined object's self-similarity. Whether the shapes measured by ε belong to the same fractal depends on whether the fractal dimension is fixed.

In physics and mathematics, the dimension of a mathematical space (or object) is informally defined as the minimum number of coordinates needed to specify any point within it. As for ordinary geometric shapes, points are 0-dimensional sets, lines are 1-dimensional sets which only have length, surfaces are 2-dimensional sets which have length and width, and cubes are 3-dimensional sets which have length, width and height. For complicated geometric forms whose details seem more important than the gross picture, fractal dimensions are applied as an index describing their complexity while the conventional Euclidean or topological

dimension shows its limitation. If the theoretical fractal dimension of a set exceeds its topological dimension, the set is considered to have fractal geometry (Mandelbrot, 2004). Unlike topological dimensions, the fractal index can take non-integer values (Sharifi-Viand et al., 2012). Multiple algorithms for calculating fractal dimension exist in fractal theory. The Hausdorff dimension, also called gauge dimension, is the most basic. Others include information dimension, correlation dimension, spectral dimension, distribution dimension and Lyapunov dimension, etc. The box-counting dimension (or Minkowski dimension) is used in this paper.

2.2.2 Calculation of box-counting dimension

Using a ruler of length ε to measure a line segment of length L, $N(\varepsilon)$ as the ratio of L to ε can be obtained. Similarly, using cubes with side length ε to fill an object, $N(\varepsilon)$ is the number of cubes required to cover the object. The fractal dimension obtained in this way is called box-counting dimension Dc (Zhu et al., 2011), and is defined as:

$$Dc = \lim_{n\to\infty}\left[\ln N(\varepsilon)/\ln(1/\varepsilon)\right] \tag{1}$$

When ε approaches 0, it becomes:

$$\ln N(\varepsilon) \approx -Dc\ln\varepsilon = Dc\ln(1/\varepsilon) \tag{2}$$

Where ε—— the scale at which the fractal is measured, Dc —— the box-counting dimension, and $N(\varepsilon)$ —— the covering number.

If there is a straight part (clear correlation) on the $\ln NN(\varepsilon)$-$\ln(\varepsilon)$ graph with linear fitting, the sequence can be conceived as a fractal. The slope of the straight part Dc is the fractal dimension. Smally (1987) introduced a new variable (NN) when computing the fractal dimension of the earthquake spectrum series of New Hebrides, namely the relative measurement:

$$NN(\varepsilon) = N(\varepsilon) / NT \tag{3}$$

Where $N(\varepsilon)$——absolute measurement, NT——total number of time intervals, T——total time length, ε——step length.

A fractal problem depends on the existence of a straight part (scale-invariant area) on the $\ln NN(\varepsilon)$-$\ln(\varepsilon)$ curve (Dong et al., 2007; Mandelbrot, 1983; Song et al., 2002; Ding et al.,

1999). If the slope of the straight part in the scale-invariant area is b, the capacity dimension can be given by the following equation:

$$Dc = d - b \tag{4}$$

Where d——topological dimension. Points of flood peaks distribute on a Q~t two-dimensional surface, so d equals to 2, and then:

$$Dc = 2 - b \tag{5}$$

2.3 Von Mises distribution method

The Von Mises method uses the Von Mises distribution to simulate the pattern of flood timing, based on which accumulative flood frequencies can be obtained and then flood season can be separated into sub-seasons.

2.3.1 Von Mises distribution

Compared with single normal distribution, the Von Mises distribution is a continuous probability distribution on a circle. This model primarily describes directional statistics. It is important in areas like astronomy, biology, geography, medicine, etc. For example, He et al. (2011) applied the Von Mises yield criterion in the study of materials in plastic state in physics; Zheng et al. (2011) applied the Von Mises distribution model of monthly premium to analyze the seasonal fluctuation of the premium in medical science. The Von Mises distribution is also applied in hydrologic events. Fang et al. (2008) employed the Von Mises function to fit the time distribution of annual maximum flood and have established a two-variable joint distribution of annual maximum flood.

The probability density curve of the Von Mises distribution is unimodal. However, the probability density curve of the time of the occurrence of floods in flood season also can be multimodal in practical calculation (Yue et al., 1999). Therefore, fitting result and actual measurement may differ when the Von Mises function is used to fit the probability distribution of flood timing. Replacing the Von Mises distribution with mixed Von Mises distribution achieved well-fitted result (Chen et al. 2010).

2.3.2 Distribution establishment and parameter calculation

Assuming flood date t is normally distributed, its probability density function is (Fang et al., 2008):

$$f(t)=\frac{1}{2\pi I_0(k)}\exp\left[k\cos(t-u)\right] \qquad 0\le t\le 2\pi, 0\le u\le 2\pi, k>0 \tag{6}$$

Where u——measure of location, k ——measure of concentration, $I_0(k)$——modified Bessel function of order 0. Assuming there are L days during flood season, N——number of flood samples, D_i——time of the occurrence of sample i, and:

$$a=\sum_{i=1}^{N}cosx_i/N \qquad b=\sum_{i=1}^{N}sinx_i/N \tag{7}$$

where $x_i=D_i\dfrac{2\pi}{L}$ is the time of the occurrence of sample i (in radians), $0\prec x_i\prec 2\pi$.

Then u and k can be given by:

$$u=\begin{cases}\arctan b/a & a>0,b>0\\ 2\pi+\arctan b/a & a>0,b<0\\ \pi+\arctan b/a & a<0\\ \pi/2 & a=0,b>0\\ 3\pi/2 & a=0,b<0\\ \text{indeterminate} & a=0,b=0\end{cases} \tag{8}$$

$$u=r=\sqrt{a^2+b^2} \qquad 0\le r\le 1 \tag{9}$$

In this study, the probability density function of t is given by:

$$f_t(t)=\sum_{i=1}^{n}\frac{p_i}{2\pi I_0(k_i)}\exp[k_i\cos(t-u_i)] \qquad 0\le t\le 2\pi, 0\le u_i\le 2\pi, k>0 \tag{10}$$

Where n is the number of Von Mises distributions, p_i is the mixing percentage, and their optimal values that produce the best fitting result can be obtained with the Quasi-Newton method (Li et al., 1997).

3 Application example

Built in 1960, Hongfeng reservoir is a large multi-year regulating storage reservoir for hydropower generation, flood control, water supply and recreation. As the leading reservoir of

the cascade of hydropower stations along Maotiao River, Hongfeng is the key to ensuring the safety of the cascade system. The watershed controlled by Hongfeng reservoir has an area of 1596 km^2, an average elevation of 1327m, and an average river bed slope of 1.21‰. The Maotiao river flood season begins in May and ends in September, and rainfall in this period of time accounts for 70% of annual inflow. Annual maximum floods typically occur in June or July. The location of Hongfeng Reservoir is shown in Fig. 1.

3.1 Flood season separation of Hongfeng reservoir

3.1.1 Application of statistical method

The flood season of Hongfeng reservoir is from May 1st to September 30th (lasting for 153 days). This study uses the historical hydrology record lasting 43 years.

Table 1 shows that the largest flood within a year appears in the first ten-day period of August, until the frequency of the largest inflow is 90.698%, while the second and the third largest flood occur in the last ten-day period of August and the first ten-day period of September, until which the frequencies of the second and the third largest inflow are 93.023% and 90.698% respectively during the whole flood record. In terms of the multi-year average and largest inflow in a ten-day period, the late July and the early August were at a low point as well as late August and early September. Therefore, the flood season of Hongfeng reservoir can be separated into three sub-seasons based on the analysis of its changing flood pattern and safety requirement. The pre-rainy season is from May 1st to July 31st, the middle flood season is from August 1st to August 31st, and the late flood season is from September 1st to September 30th.

3.1.2 Application of fractal method

Earlier researches only sampled the sequence of the largest daily inflows, while this paper also accounts for the second and the third largest daily inflows. Distributions of the three largest daily inflows are shown in Fig. 2.

The first three largest daily inflow series in a 43-year research period are adopted as research sample and thus 43 points form a series. Note that there are some years in which the largest daily inflows are lower than the second largest of latter years, and they occurred on very near dates in different years, so some parts of the three series are tangled. Figure 2 shows large gaps between the ten-day period inflows of May and June, July and August, and August and

September. So the flood season can be divided into four sub-seasons. Time scale ε is 1d, 2d, 3d... 7d, or 8d. By setting a fixed value $Y1=235m^3/s$ (slightly larger than the sample average inflow), $N(\varepsilon)$ can be obtained under different time scales by counting the number of time intervals in which the average inflows exceed $Y1$(Fig. 3-(1)). The $\ln NN(\varepsilon)$-$\ln(\varepsilon)$ graph can be plotted to determine slope b of the straight part and then obtain the box-counting dimension Dc ($Dc=2-b$). Different $\ln NN(\varepsilon)$-$\ln(\varepsilon)$ graphs can be plotted based on different values of T when changing the ending date of the first sub-season. Calculation of the latter three sub-seasons is similar to the first sub-season, and the average inflows are as $Y2=540m^3/s$(Fig. 3-(2)), $Y3=265m^3/s$(Fig. 3-(3)), $Y4=235m^3/s$(Fig. 3-(4)) respectively. The $\ln NN(\varepsilon)$-$\ln(\varepsilon)$ graphs under different values of T of the four sub-seasons are shown in Fig. 3.

Shi et al., (2010) suggest that the significant linear relation between $\ln NN(\varepsilon)$ and $\ln(\varepsilon)$ is inversely proportional to the length of the time scale ε and thus should not exceed 6. This case achieves the best result when ε is 8. The calculated box-counting dimensions of the four sub-seasons are shown in Table 2. From Table 2, the box-counting dimensions of situation A and situation B have a slight difference of 0.01 in the pre-rainy season, while situation C largely differs. According to the principle that the box-counting dimensions in the same sub-season should have similar magnitudes while successive sub-seasons do not, A and B should belong to the same sub-season. So it can be concluded that the pre-rainy season is from May 1st to May 31st. Similarly, the box-counting dimensions of situation D, E and F are close with a relative difference less than 4% in the main flood season, while G is rather different. So the main flood season is from June 1st to July 31st. In the late-flood season I, there is a discontinuous part due to the comparatively large difference between the box-counting dimensions of situation I and situations H and J. So situation H is regarded as one sub-season and the late-flood season I is from August 1st to August 31st. Under such circumstance, the late-flood season in the conventional sense is divided into two sub-seasons, including the late-flood season I and the late-flood season II. In the late-flood season II, situation M is counted out because October is not included in the flood season. It can only be concluded that the late-flood season II is from September 1st to September 20th, and the remaining ten days until September 30th should be regarded as another sub-season if the fractal principle is strictly followed. However, to make it convenient for reservoir management and operation, the late-flood season II should be from September 1st to September 30th.

The above separation was based on the sequence of the largest daily inflows. The separation results based on the sequences of the second and third largest daily inflows are similar, which proves that taking sequence of only the largest daily inflows as research sample is reasonable for separation

3.1.3 Application of the mixed Von Mises distribution

Due to the scarce inflow records of Hongfeng reservoir, more reasonable flood peak records were adopted as samples to accurately trace changes in floods to make the distribution model more relevant. Based on Peaks-Over-Threshold (POT) sampling, this study selected 156 Peaks-Over-Threshold (POT) floods from Hongfeng's 43-year inflow records and two historical catastrophic floods in May 1830 and August 1892 with a threshold of 160 m^3/s. The selected sample floods satisfy the principles of independence and uniformity. A mixed Von Mises distribution with three parts (n=3) was then established. Relevant parameters are u1=0.50, k1=27.53, P1=0.10; u2=2.28, k2=2.82, P2=0.66; u3=0.48, k3=3.05, P3=0.24. Given these parameters, the density function of this mixed Von Mises distribution are:

$$f_1(t) = \frac{1}{2\pi} \times \frac{0.10}{6.89 \times 10^{-10}} \exp\left[27.53\cos(t - 0.50)\right]$$

$$f_2(t) = \frac{1}{2\pi} \times \frac{0.66}{4.22} \exp\left[2.82\cos(t - 2.28)\right]$$

$$f_3(t) = \frac{1}{2\pi} \times \frac{0.24}{5.10} \exp\left[3.05\cos(t - 0.48)\right]$$

$$f_t(t) = f_1(t) + f_2(t) + f_3(t) \quad (11)$$

According to the above formulas, the fitting graph for the mixed Von Mises distribution of the floods occurring time is plotted in Fig. 4.

As shown in Fig. 4, floods in Maotiao River mainly occur in June and July and sometimes in the middle of May, August and September. Floods in May, August and September account for 16%, 15% and 8% respectively of all floods in flood season, while floods in June and July are 61% of all floods. The Maotiao River flood season is characterized with sub-seasons. In addition, the hydrologic records show that runoff in Maotiao River changes slightly from year to year but largely changes within one year. The largest annual flood generally occurs before August, mostly in June or July. Based on the selected sample sequence, two sub-season

definitions were proposed. Both strategies have May as the pre-rainy season, June and July as the main flood season. But one has August as the late-flood season I and September as the late-flood season II, while another combines August and September into one late-flood season. This paper shows that the theoretical curve based on the latter strategy can better fit the sample sequence, and apparently the mixed Von Mises distribution under such circumstance has three parts (n=3). As is seen in Fig.4, there is a roughly ten-day lag between the theoretical Von Mises curve and the observations' frequencies during June, but it has little impact on the flood season separation because what matters most is in which period flood is the most prone to occur, and June and July are combined into one sub-season.

3.2 Analysis on flood control levels of different sub-seasons for Hongfeng reservoir

According to Design Report of Cascade Hydropower Station in Maotiao River released in 1987 by the Ministry of water resources and Guiyang Engineering Corporation, the flood control level of Hongfeng reservoir was set at 1236.0m, the highest reservoir water level and the maximum discharge for the 100-yr design flood were 1239.97m and 1420m^3/s respectively, and for the 5000-yr check flood were 1242.58m and 2450m^3/s respectively.

This paper used two new methods for developing flood sub-seasons and thus different methods for design flood calculation. The fractal method used sampling of annual largest values to calculate design floods of all sub-seasons by the same-frequency amplification method, while the mixed Von Mises distribution used POT sampling to establish the joint distribution of peak flow and occurring time of floods based on two-dimensional Frank Copula function to calculate the design floods. Peak flows of the 100-yr (1% frequency) design flood and 5000-yr (0.02% frequency) check flood of different sub-seasons from the above two methods are shown in Table 3.

According to the separation result, this paper selected the flood in May 1996 for the pre-rainy season, two floods in July 1991 and July 1996 for the main flood season, the flood in August 2000 for the late-flood season I and the flood in September 1970 for the late-flood season II as typical sequence of floods. For the sub-seasons with the mixed Von Mises distribution, flood in August 2000 was selected as a typical flood for the late-flood season. Three flood operating rules were applied to the design floods calculated from different typical floods, specifically open-discharge strategy, strategy for operating in 1987 and strategy for check in

1990. Operating results with the mixed Von Mises distribution sub-seasons are shown in Table 4.

As shown in Table 4, the highest adjusted water levels vary for typical floods in different sub-seasons. The main flood season is featured with a lower initial water level due to its higher inflow volume, but still higher than the previously determined 1236.0m. For different design flood standards, the highest reservoir water levels from the above calculation are 1240.0m and 1242.58m, and the largest discharge flows are 1420.0 m^3/s and 2450.0m^3/s.

Flood control level changes with flood sub-seasons. Flood control levels in the pre-rainy season and the late-flood season are higher than that of the main flood season, which increases the operating water level of Hongfeng reservoir in the whole flood season. In addition, the reservoir could release surplus water later and store more water for drought after the flood season. Due to the lack of data, calculating the design flood based on rainfall data was not carried out. For safety, this paper adjusted the calculated flood control levels and the final result is close to the research done by Li (2007). Flood control levels of Hongfeng reservoir in different sub-seasons with three methods are shown in Fig. 5. Based on the flood regulating calculations in sub-seasons, the range of flood control level in each sub-season is obtained with the fixed flood control level of the original plan as the lower limit. As is seen in Fig.5, there is a raise of the flood control level in each sub-season and with different methods for separation comes different flood regulation calculations and thus flood control level is raised to different extents. More clearly, table 5 shows the deferent operating level of Hongfeng reservoir in the different stages in flood season for the three methods. . Based on the flood regulating calculations in sub-seasons, the range of flood control level in each sub-season is obtained with the fixed flood control level of the original plan as the lower limit. As is seen in Table 5, there is a raise of the flood control level in each sub-season and with different methods for separation comes different flood regulation calculations and thus flood control level is raised to different extents.

Evenmore, with the separation results reservoir operation calculation is conducted and the results of electricity generation under dynamic control of flood control level are shown in Table 6. Comparing with the original plan with a fixed flood control level at 1236m and the actual case, the electricity generation under the separation of flood season with the three methods has all increased to various degrees, showing sub-season method can increase the output, so as to obtain more economic benefits.

4 Conclusions

The aim of the separation of flood season of reservoir is to make better flood regulation schemes, which can make better use of the surplus water in flood season and increase benefits, such as by generating more electricity, without extra construction cost. Therefore, the statistical development of flood frequencies for sub-seasons within the annual flood season has potential to improve multipurpose reservoir system operation. This paper is mainly concerned about the separation of flood season, yet it also has a lot to do with the dynamic control of flood control level in flood season. Dynamic control of flood control level in flood season is an emerging field in which relevant researches are scarce, due to the deep-rooted conventional mindset that flood control level should be fixed in the whole flood season. But there still are some researchers who have done much work, such as Zhou et al. (2014); Yun and Vijay (2008); Li et al. (2010); Jiang et al. (2015). However, how to implement real-time reservoir FLWL dynamic control is a future challenge.

Applying the three methods to the separation of the flood season of Hongfeng Reservoir in the case study, this paper then accordingly conducts flood regulation calculation under three different regulation strategies. Based on the flood regulation calculation in sub-seasons, the different ranges of flood control level in each sub-season are obtained with the fixed flood control level of the original plan as the lower limit. Under the requirement of flood control safety, adopting the new operation schemes can help increase the total benefits of reservoir, especially in electricity generation and water supply, etc.

a. With long-term flood record, the conventional statistical method can be used for flood season separation through frequency calculation. The fractal theory is applicable to flood series featured with randomness，nonlinearity，determinacy and similarity. In this paper, by using the first three largest sequences of daily inflow as research samples for the fractal method, so it only revealed statistics of extreme values. A POT (Peaks-Over-Threshold sampling) method was used to select samples for the mixed Von Mises distribution method, which achieves the independence of flood sample and makes up for short flood records. Therefore, results based on POT method can reflect the rules of flood occurrence.

b. On the whole, the separation results from the fractal theory and mixed Von Mises distribution are similar to the conventional method. As reservoir operation becomes more

difficult with more flood sub-seasons, the mixed Von Mises distribution method achieves a more reasonable result.

Acknowledgements

This study was financially supported by the CRSRI Open Research Program (Program SN: CKWV2015232/KY) and National Natural Science Foundation of China (No.41340022). There are special thanks to Professor Jay R. Lund and Hui Rui from University of California, Davis who gave many helpful comments on this paper.

References

Cao Yongqiang. Study on floodwater utilization and management. Resources & Industry, vol.6, no.2, pp.21-23, 2004.

Chen Shouyu. Methodology of fuzzy sets analysis to hydrologic system from research on flood period description. Advances in Water Science, vol.6, no.2, pp. 133-138, 1995.

Liu Pan, Guo Shenglian, Wang Caijun. Flood season staged for three gorges reservoir based on the change-point approach. Hydrology, vol.25, no.1, pp.18-23, 2005.

Pan Liu, Liping Li, Shenglian Guo, Lihua Xiong, Wang Zhang, Jingwen Zhang, Chong-Yu Xu. Optimal design of seasonal flood limited water levels and its application for the Three Gorges Reservoir. Journal of Hydrology, 527, 1045–1053, 2015.

Hou Yu, Wu Boxian, Zheng Guoquan. Preliminary study on the seasonal period's classification of floods by using fractal theory. Advance in Water Science, vol.10, no.2, pp. 140-143, 1999.

Fang Bin, Guo Shenglian, Liu Pan, Xiao Yi. Advance and Assessment of Seasonal Design Flood Methods. Journal of Hydroelectric Power, vol.33, no 7, pp. 71-75, 2007.

Fang Bin, Guo Shenglian, Xiao Yi, Liu Pan, Wu Jian. Annual maximum flood occurrence dates and magnitudes frequency analysis based on bivariate joint distribution. Advance in Water Science, vol.19, no.2,pp. 505-511, 2008

Wei wei, Mo Chongxun, Liu Li, Jiang Qingling et al. Application of Watershed Rainfall Fractal Theory in Reservoir Flood Season Staging. Yellow River, vol.36, no.10, pp.39-41, 2014.

Chen Lu, Guo Shenglian, Yan Baowei, Liu Pan. A new seasonal design flood estimation method. Engineering Journal of Wuhan University, vol.43, no 1, pp. 20-24, 2010.

Liu Ying, Hu Min, Yu Guiying, Li Xiaobing. Theory of Fractal and its Applications. Jiang Xi Science, vol.24, no.2, pp. 205-209, 2006.

Zhang Shaowen, Wang Wensheng, Ding jin, Chang Fuxuan. Application of Fractal Theory to Hydrology and Water Resources, Advance in Water Science, vol.16, no.1, pp. 141-146, 2009.

Zhang Jiansheng, Huang Qiang, Ma Yongsheng etc. Division of flood seasonal phases for reservoir and the evaluation method. Journal of Northwest A&F University (Nat. Sci. Ed.), vol.37, no.10, pp. 229-234, 2009.

Mandelbrot, B. B. Fractals and chaos. Springer Berlin, 32(2), xii,308, 2004.

Sharifi-Viand, A., Mahjani, M. G., & Jafarian, M. Investigation of anomalous diffusion and multifractal dimensions in polypyrrole film. Journal of Electroanalytical Chemistry, 671(8), 51-57, 2012.

Zhu Hua, Ji Cuicui. Fractal theory and its applications. Science publishing house, Beijing (in Chinese), pp.42-45, 2011.

Smally R F. A Fractal Approach to The Clustering of Earth Quakes: Application to The Simplify of The New Hebrides. BSSA, vol.27, no.4, pp. 32-49, l987.

Dong Qianjin, Wang Xianjia, Wang Jianping, Fu Chun. Application of Fractal Theory in The Stage Analysis of Flood Seasons in Three Gorges Reservoir. Resources and Environment in the Yangtze Basin, vol.16, no.3, pp. 400-404, 2007.

Mandelbrot B B. The Fractal Geometry of Nature.San Francisco: Freeman, 1983.

Song Lisong. Analyses on Sudden Change in Low Tide Level Series of the Caoe River. Journal of Sediment Research, no.1, pp. 69-71, 2002.

Ding jing, Liu Guodong. Estimation of Fractal Dimension for Daily Flow Hydrograph. Si Chuan Water power, vol.18, no.4, pp. 74-76, 1999.

He Linwei, Cai Guoping. A Bi-directional Optimization Method for Continuous Structures Subject to Von Mises Stress Constraints. Chinese Quarterly of Mechanics, vol.32, no.1, pp.

19-26, 2011.
Zheng Yu, Zhang Juan, Yang Huawei. Application of Von Mises Distribution in Insurance Premium in Shaanxi Province. Statistics & Information Forum, vol.26, no.1, pp. 28-30, 2011.
Fang Bin, Guo Shenglian, Xiao Yi etc. Annual maximum flood occurrence dates and magnitudes frequency analysis based on bivariate joint distribution. Advances in Water Science, vol.19, no.4, pp. 506-511, 2008.
S. Yue，T.B.M.J. Ouarda, B. Bobe´e, P. Legendre, P. Bruneau. The Gumbel mixed model for flood frequency analysis. Journal of Hydrology, pp.88-100, 1999.
Li Yuansheng. The direction of statistics. China science and technology publishing house, Beijing (in Chinese), pp.129-131, 1997.
Shi Yuezhen, Li Miao, Zheng Yangqi. Flood season staged in Xiangjiang river basin based on fractal theory [J]. Bulletin of Soil and Water Conservation, vol.30, no.5, pp. 165-167, 2010.
Li Jiqing, Ji Changming, Lu Qiyou. Flood control limited level of Hongfeng reservoir during the former flood season [J]. Journal of North China Electric Power University, vol.34, no.4, pp. 27-31, 2007.
Yanlai Zhou, Shenglian Guo, Pan Liu, Chongyu Xu. Joint operation and dynamic control of flood limiting water levels for mixed cascade reservoir systems, Journal of Hydrology, 519 248–257, 2014.
Ruan Yun, Vijay P. Singh. Multiple duration limited water level and dynamic limited water level for flood control with implications on water supply, Journal of Hydrology, 354, 160–170, 2008.
Xiang Li, Shenglian Guo, Pan Liu, Guiya Chen. Dynamic control of flood limited water level for reservoir operation by considering inflow uncertainty, Journal of Hydrology, 391, 124–132, 2010.
Zhiqiang Jiang, Ping Sun, Changming Ji, Jianzhong Zhou. Credibility theory based dynamic control bound optimization for reservoir flood limited water level, Journal of Hydrology, 529, 928–939, 2015.

Table 1. Frequency of the Occurence of the First Three Largest Peak Flows.

Month	Ten-day period	Annual largest peak flow		second largest peak flow		Third largest peak flow	
		Distribution of frequency	Cumulative Frequency (%)	Distribution of frequency	Cumulative Frequency (%)	Distribution of frequency	Cumulative Frequency (%)
April	1st -10th	0		0		0	
	11th-20th	0		1	2.326	0	
	21th-30th	0		0		0	
May	1st -10th	0		3	9.302	1	2.326
	11th-20th	1	2.326	3	16.279	4	11.628
	21th-31st	2	6.978	1	18.605	5	23.256
June	1st -10th	4	16.279	3	25.581	5	34.884
	11th-20th	9	37.216	6	39.535	5	46.512
	21th-30th	10	60.465	6	53.488	6	60.465
July	1st -10th	4	69.767	7	69.767	2	65.116
	11th-20th	3	76.744	3	76.744	5	76.744
	21th-31st	5	88.372	1	79.070	3	83.721
Aug.	1st -10th	1	90.698	2	83.721	1	86.047
	11th-20th	1	93.023	2	88.372	1	88.372
	21th-31st	0		2	93.023	0	
Sep.	1st -10th	0		0		1	90.698
	11th-20th	0		3	100	3	97.674
	21th-31st	1	95.366	0		0	
Oct.	1st -10th	0		0		1	100
	11th-20th	1	97.674	0			
	21th-31st	1	100	0			
total		43	100	43	100	43	100

Table 2. Box-counting Dimensions of Different Flood Sub-seasons.

sub-seasons	situation	time length *T*	starting date (d/m)	ending date (d/m)	Correlation coefficient *R*	Slope *b*	*Dc*
Pre-rainy season	A	20	1st May	20th May	0.97	0.29	1.71
	B	31	11th May	31st May	0.95	0.30	1.70
	C	42	21th May	1st July	0.93	0.42	1.58
Main flood season	D	40	1st June	20th July	0.92	0.44	1.56
	E	50	1st June	20th July	0.96	0.43	1.57
	F	61	1st June	31st July	0.97	0.40	1.60
	G	71	1st June	10th Aug.	0.97	0.28	1.72
Late flood season I	H	31	1st Aug.	31st Aug.	0.96	0.46	1.54
	I	41	1st Aug.	10th Sept.	0.97	0.38	1.62
	J	51	1st Aug.	20th Sept.	0.97	0.44	1.56
Late flood season II	K	20	1st Sept.	20th Sept.	0.98	0.49	1.51
	L	30	1st Sept.	30th Sept.	0.97	0.39	1.61
	M	40	1st Sept.	10th Oct.	0.97	0.38	1.62

Table 3. Peak Flows of Design Floods of Different Sub-seasons.

method	Frequency/%	Annual largest flow /$m^3 \cdot s^{-1}$	Pre-rainy season/$m^3 \cdot s^{-1}$	Main flood season /$m^3 \cdot s^{-1}$	Late flood season	
					I	II
frequency method	1	1886.0	534.0	2595.5	771.0	570.17
	0.02	3586.8	663.6	3782.9	1021.4	777.49
copula function	1	1886.0	1559.7	2089.7	1436.5	1436.5
	0.02	3586.8	3111.3	3641.7	2846.2	2846.2

Table 4. Results of Flood Regulation with the Mixed Von Mises Distribution.

Frequency (%)	Sub-seasons	Typical design flood	Initial water level /m	Scheme 1		Scheme 2		Scheme 3	
				highest water level /m	maximum discharge / $m^3 \cdot s^{-1}$	highest water level /m	maximum discharge / $m^3 \cdot s^{-1}$	highest water level /m	maximum discharge / $m^3 \cdot s^{-1}$
1	1st May - 31st May	"96.5"	1239.4	1240.0	1396.3	1240.0	1399.6	1240.0	1383.2
	1st June	"91.7"	1238.3	1240.0	1391.2	1240.0	1391.0	1240.0	1391.0
	-31st July	"96.7"	1236.8	1240.0	1396.7	1240.0	1432.7	1240.0	1432.7
	1st Aug. -30th Sept.	"00.8"	1239.9	1240.0	1368.7	1240.0	1370.8	1240.0	1368.5
0.02	1st May -31st May	"96.5"	1240.7	1242.5	2390.9	1242.5	2394.0	1242.5	2395.1
	1st June	"91.7"	1241.1	1242.5	2392.3	1242.5	2410.6	1242.5	2410.6
	-31st July	"96.7"	1237.8	1242.5	2403.3	1242.5	2406.1	1242.5	2395.4
	1st Aug -30th Sept	"00.8"	1241.5	1242.5	2405.5	1242.5	2407.5	1242.5	2405.4

Table 5. Ranges of Flood Control water Level in Flood Season with Different Methods

(unit: m)

	May	June	July	August	September
original plan	1236.0				
conventional statistical method	1236.0 - 1236.8			1236.0 - 1239.1	1236.0 - 1239.4
fractal method	1236.0 - 1238.0	1236.0 - 1236.8		1236.0 - 1239.5	1236.0 - 1239.7
Von Mises Distribution method	1236.0 - 1239.1	1236.0 - 1236.8		1236.0 - 1239.6	1236.0 - 1239.6

Table 6. Increase of Electricity Generation with Three Separation Methods over the Original Plan and the Actual Case

	Original plan	Actual case	Conventional statistical method	Fractal method	Von Mises method
Electricity generated (10^4 Kw*h)	6273	6053	6611	6625	6628
Absolute increase over the original plan (10^4 Kw*h)	/	/	238	252	255
Increase in percentage over the original plan	/	/	3.73%	3.95%	4.00%
Absolute increase over the actual case (10^4 Kw*h)	/	/	558	572	575
Increase in percentage over the actual case	/	/	9.22%	9.45%	9.50%

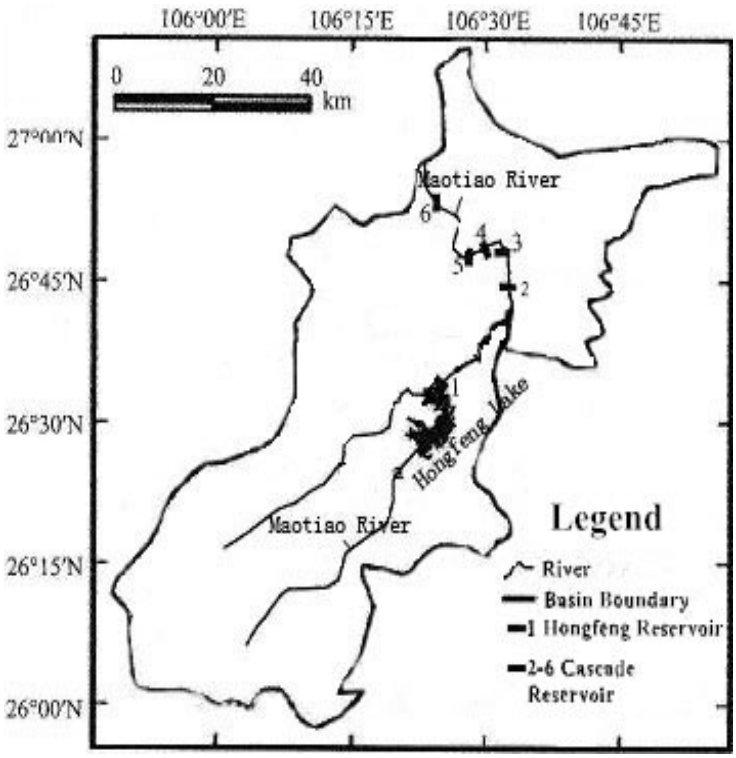

Figure 1. The location of Hongfeng Reservoir.

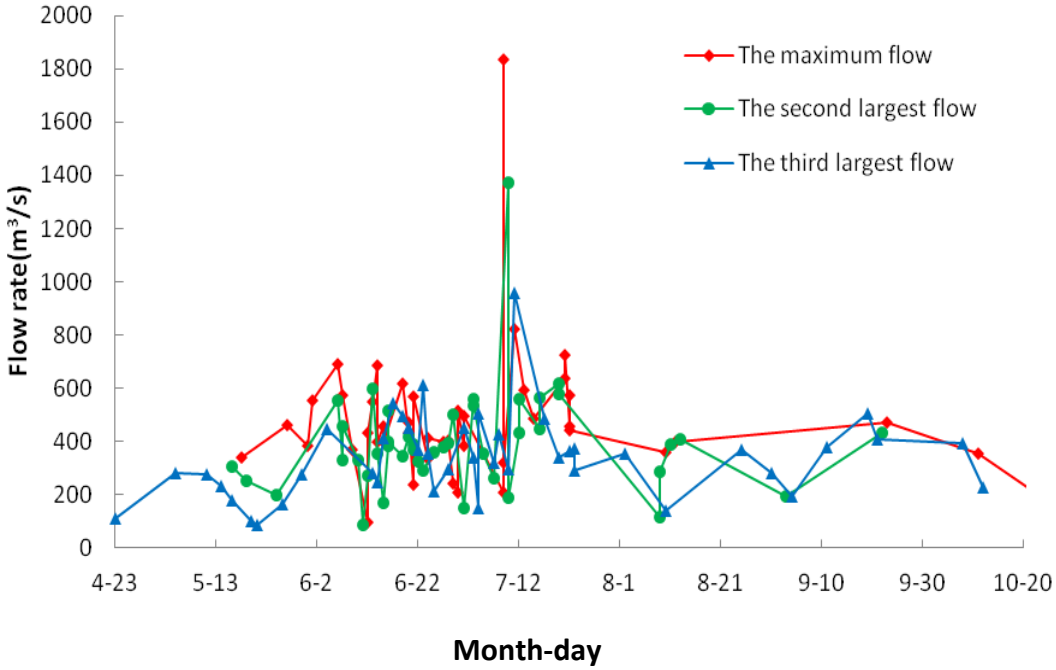

Figure 2. Distributions of the three largest daily inflows.

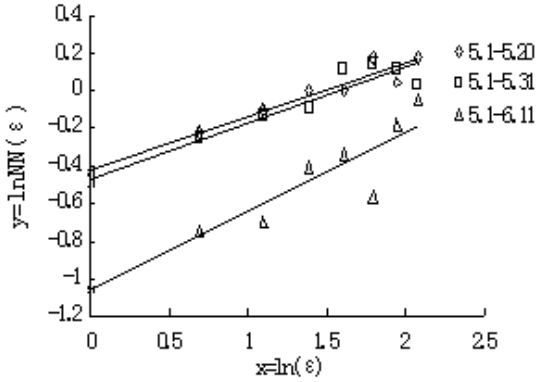

(1) $Y1$=235m^3/s

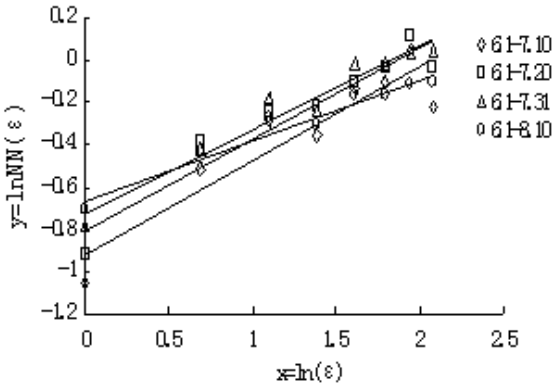

(2) $Y2$=540m^3/s

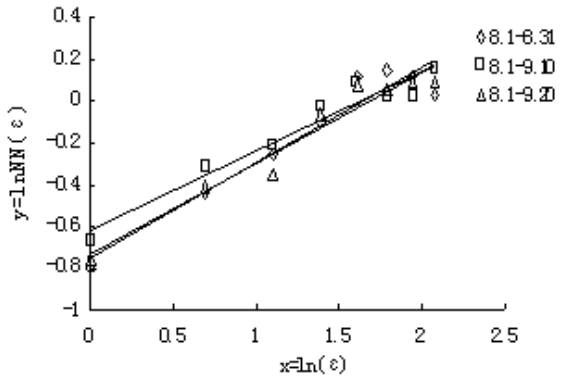

(3) $Y3$=265m^3/s

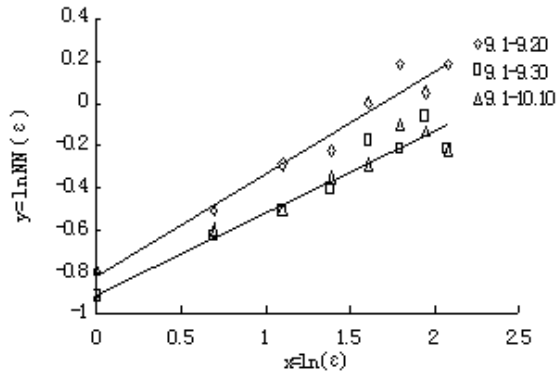

(4) $Y4$=235m^3/s

Figure 3. Relationship between *NN(ε)* and *ε* with logarithmic coordinates.

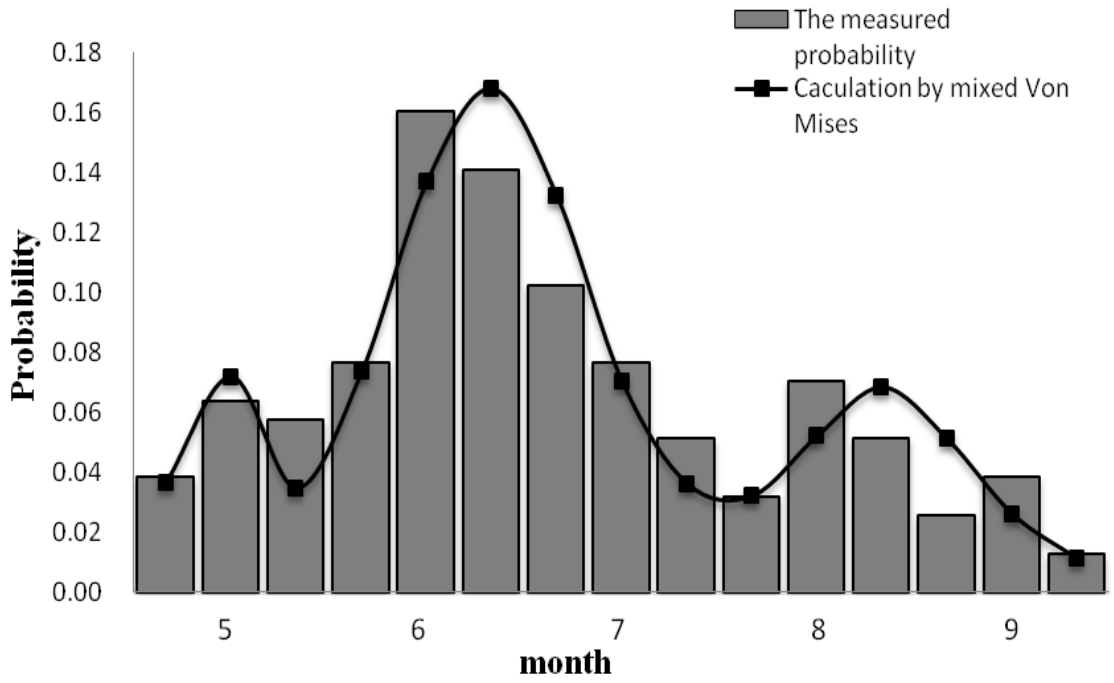

Figure 4. Probability of flood flow.

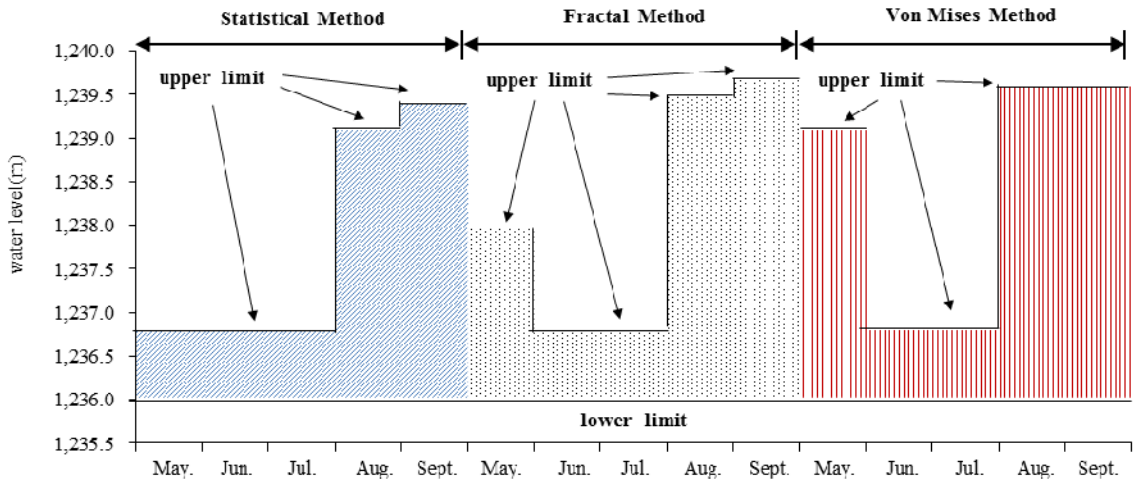

Figure 5. Results of flood control levels of Hongfeng Reservoir by sub-seasons with three methods.